Sukhrob Abdulazhanov

Design, Integration and Characterization of CMOS-compatible RF Varactors Based on Ferroelectric HfO2 Thin Films

TUDpress

DRESDNER BEITRÄGE ZUR SENSORIK

Herausgegeben von

Gerald Gerlach

Band 95

Sukhrob Abdulazhanov

Design, Integration and Characterization of CMOS-compatible RF Varactors Based on Ferroelectric HfO2 Thin Films

TUD*press*

2025

Die vorliegende Arbeit wurde unter dem Titel „Design, integration and characterization of CMOS-compatible RF varactors based on ferroelectric HfO2 thin films" am 05.05.2024 als Dissertation an der Fakultät Elektrotechnik und Informationstechnik der Technischen Universität Dresden eingereicht und am 04.11.2024 verteidigt.

Vorsitzender:	Prof. Dr.-Ing. Thomas Mikolajick
Gutachter	Prof. Dr.-Ing. habil. Gerald Gerlach Prof. Dr. Lambert Alff
Weiteres Mitglied:	Prof. Dr. rer. nat. Johann Wolfgang Bartha

Bibliografische Information der Deutschen Nationalbibliothek
Die Deutsche Nationalbibliothek verzeichnet diese Publikation in der Deutschen Nationalbibliografie; detaillierte bibliografische Daten sind im Internet über http://dnb.d-nb.de abrufbar.

Bibliographic information published by the Deutsche Nationalbibliothek
The Deutsche Nationalbibliothek lists this publication in the Deutsche Nationalbibliografie; detailed bibliographic data are available in the Internet at http://dnb.d-nb.de.

ISBN 978-3-95908-823-7

Thelem Universitätsverlag und
Buchhandlung GmbH & Co. KG
Dresden und München
Tel.: 0351/472 14 63 | Fax: 0351/479 69 721
http://www.tudpress.de

TUDpress ist ein Imprint von Thelem.

Gesetzt vom Autor.
Printed in Germany.

Editor's Preface

For many years, there has been a goal to develop non-volatile memory devices based on ferroelectric materials. Initially, research focused primarily on lead zirconate titanate (PZT). However, PZT failed to gain acceptance due to its lack of scalability and the difficulty of integrating lead into the CMOS semiconductor process. In 2011, a group led by Böscke (Qimonda) and Müller (Fraunhofer CNT and IPMS) published a paper which reported the formation of crystalline phases exhibiting ferroelectric behavior in thin layers of SiO_2-doped hafnium oxide (HfO_2). The occurrence of ferroelectricity (FE) in HfO_2 is remarkable because it is one of the few metal oxides that can be thermodynamically stably deposited on silicon. This publication already predicted that Si-FE transitions could form the basis not only for non-volatile memory in microelectronics but also for many other components.

In the few years since that discovery, HfO_2 has become the subject of extensive research. Particular focus has been given to classical applications in memory devices like ferroelectric field-effect transistors (FeFETs), and the use of such devices in in-memory and neuromorphic computing. Other applications include energy harvesting systems, pyroelectric sensors and components for electrocaloric cooling.

In his dissertation, Sukhrob Abdulazhanov turns his attention to another class of electronic devices that use HfO_2-integrated, CMOS-compatible thin films: varactors. These are components in which a change in the applied voltage can be used to achieve a change in capacitance. This is important for tuning resonant circuits at high frequencies, such as filters and oscillators, or for adjusting the frequency in radio receivers.

In particular, the author investigates varactors based on hafnium zirconium oxide (HZO) as metal-ferroelectric-metal (MFM) stacks in the Back-End-of-Line of the CMOS manufacturing process. In doing so, he thoroughly and systematically examines the influence of doping, layer thickness, temperature, and alternating electric fields on the dielectric constant and dielectric loss of HZO, as well as the varactors' tuning properties. Parameters of particular interest include the broadband properties and the achievable phase shift. Finally, he designed, fabricated, and characterized various passive circuits with MFM varactors.

The work presented here thus addresses an extremely important scientific and technical issue. It lays the foundation for the future application of HZO in CMOS-based integrated varactor devices, which could also have significant economic implications. The significance of this work can therefore be considered fundamental. For this reason, I am confident that this volume of the book series "Dresden Contributions to Sensor Technology" will receive the attention it fully deserves.

Dresden, July 2025
Gerald Gerlach

TECHNISCHE UNIVERSITÄT DRESDEN

Design, Integration and Characterization of CMOS-compatible RF Varactors Based on Ferroelectric HfO_2 Thin Films

Dissertation

zur Erlangung des akademischen Grades

Doktor - Ingenieur
(Dr. -Ing.)

vorgelegt von

Abdulazhanov Sukhrob
geboren am 19. September 1994 in Duschanbe, Tadschikistan

Fakultät Elektotechnik und Informationstechnik
Institut für Festkörpereletktronik
TU Dresden

Eingereicht am 05.05.2024
Erster Gutachter: Prof. Dr.-Ing. habil. Gerald Gerlach
Zweiter Gutachter: Prof. Dr. Lambert Alff
Dritter Gutachter: Dr. habil. Thomas Kämpfe

Abstract

Thin film varactors are widely used in modern radio frequency integrated circuits (RFICs), in matching networks, phase shifters, voltage-controlled oscillators (VCOs) and tunable filters. Ferroelectric hafnium oxide, discovered just 10 years ago, opened a whole new research direction. Compared to other ferroelectric materials, it has a decisive advantage for use in microelectronic systems and industrial complementary-metal-oxide-semiconductor-(CMOS-) compatible production as it has been used as a gate oxide in field-effect transistors (FETs) for more than a decade. When deposited as a thin film and doped with various materials, particularly zirconium, it can crystallize at temperatures suitable for its integration into industrial Back-End-of-Line (BEoL) processes. As such, it has been extensively studied as a material for ferroelectric random-access memory (FRAM) devices. These properties also make it a perfect candidate for its implementation as a ferroelectric varactor.

In this work, a comprehensive study on metal-ferroelectric-metal (MFM) thin film varactors of hafnium oxide is carried out. It can be divided into two distinct paths - an investigation of the material properties of Zr-doped hafnium oxide and an investigation of its applicability as a varactor, where its property of tunable permittivity (or capacitance) was used to simulate, design and characterize passive elements such as phase shifters and demonstrate the advantages of the material over competing technologies. For the initial analysis of its properties, extensive measurements were made at low frequencies, particularly *I-V*, *P-V* and *C-V* characteristics. During this, the main focus was put on the influence of composition (doping), thickness, temperature and electrical treatment upon capacitance tunability. It was found that 3:5 Hf:Zr - doped thin-film varactors of 10 nm thickness have the best performance in terms of both tunability and quality factor at temperatures up to 200°C.

Additionally, the broadband characteristics was conducted using a Linear Network Analysis. The influence of doping was also analyzed for RF frequencies up to 500 MHz, where the properties were comparable to low-frequency characterization. Also, the effective permittivity and loss tangent of BEoL-integrated 10 nm hafnium zirconium oxide with 1:1 doping was extracted in the frequency range between 30 MHz and 170 GHz.

Finally, passive devices, particularly a phase shifter and a bandpass filter, were designed and integrated into the BEoL of 180 nm CMOS technology. The phase shifter demonstrates a phase shift up to 112° at 60 GHz with 41.3 dB insertion loss and 43.5° at 45 GHz with 14 dB insertion loss. The bandpass filter demonstrates the tuning of the center frequency between 36.6 GHz and 39.1 GHz with 3.87 dB insertion loss.

Kurzfassung

Dünnfilmvaraktoren werden in modernen integrierten Hochfrequenzschaltungen, Anpassungsnetzwerken, Phasenschiebern, spannungsgesteuerten Oszillatoren und steuerbaren Filtern eingesetzt. Die Ferroelektrizität in Hafniumoxid, die erst vor 10 Jahren entdeckt wurde, eröffnet hierbei eine völlig neue Forschungsrichtung. Im Vergleich zu anderen ferroelektrischen Materialien hat es einen entscheidenden Vorteil bei der Anwendung in mikroelektronischen Systemen und in der industriellen Komplementär-Metalloxid-Halbleiter- (CMOS-) kompatiblen Produktion, da es bereits seit über einem Jahrzehnt als Gate-Oxid in Feldeffekttransistoren (FETs) verwendet wird. Wenn es als Dünnfilm abgeschieden und mit verschiedenen Materialien, insbesondere Zirkonium, dotiert wird, kann es bei Temperaturen kristallisieren, die für die Integration in industrielle Back-End-of-Line-Prozesse (BEoL) geeignet sind. Daher wurde es ausgiebig als Material für ferroelektrische Direktzugriffsspeicher (FRAM) untersucht. Diese Eigenschaften machen es auch zu einem perfekten Kandidaten für seine Anwendung als ferroelektrischer Varaktor.

In dieser Arbeit wird eine umfassende Studie über Metall-Ferroelektrik-Metall (MFM)-Dünnschichtvaraktoren aus Hafniumoxid durchgeführt. Sie lässt sich in zwei verschiedene Richtungen unterteilen - eine Untersuchung der Materialeigenschaften von Zr-dotiertem Hafniumoxid und eine Untersuchung seiner Anwendbarkeit als Varaktor, bei der seine Eigenschaft der steuerbaren Permittivität (oder Kapazität) genutzt wurde, um passive Bauelemente zu entwerfen, zu simulieren und zu charakterisieren und die Vorteile des Materials gegenüber konkurrierenden Technologien aufzuzeigen. Die konventionelle Art der Analyse der ferroelektrischen Eigenschaften bei niedrigen Frequenzen, vor allem I-V-, P-V- und C-V-Kennlinien, war für die anfängliche Analyse der Eigenschaften erforderlich. Dabei lag das Hauptaugenmerk auf dem Einfluss von Zusammensetzung (Dotierung), Dicke, Temperatur und elektrischer Behandlung auf die Abstimmbarkeit der Kapazität. Es wurde festgestellt, dass 3:5 Hf:Zr - dotierte Dünnschichtvaraktoren mit einer Dicke von 10 nm die beste Leistung sowohl hinsichtlich der Abstimmbarkeit als auch des Qualitätsfaktors bei Temperaturen bis zu 200°C aufweisen.

Darüber hinaus wurden die Breitband-Eigenschaften mithilfe einer linearen Netzwerkanalyse untersucht. Der Einfluss von Dotierung wurde auch für die Frequenzen bis 500 MHz analysiert, wobei die Eigenschaften mit der Charakterisierung für niedrige Frequenzen vergleichbar waren. Außerdem wurden die effektive Dielektrizitätskonstante und der Verlusttangens von BEoL-integrierten 10 nm Hafnium-Zirkonium-Oxid mit 1:1-Dotierung im Frequenzbereich zwischen 30 MHz und 170 GHz extrahiert.

Schließlich wurden passive Schaltungen, insbesondere Phasenschieber und Bandpassfilter, entworfen und ins BEoL der 180 nm CMOS-Technologie integriert. Der Phasenschieber zeigt eine Phasenverschiebung von bis zu 112° bei 60 GHz mit 41,3 dB Einfügedämpfung und 43,5° bei 45 GHz mit 14 dB Einfügedämpfung. Das Bandpassfilter hat dabei die Abstimmung der Mittenfrequenz zwischen 36,6 GHz und 39,1 GHz mit 3,87 dB Einfügungsdämpfung.

List of Abbreviations

5G	5th generation mobile network
6G	6th generation mobile network
AFE	antiferroelectric
ALD	atomic layer deposition
BCZT	barium calcium zirconate titanate
BEoL	back-end-of-line
BiCMOS	bipolar CMOS
BPF	bandpass filter
BST	barium strontium titanate
BZN	bismuth zinc niobate
CAD	computer-aided design
CMOS	complemetary metal-oxide-semiconductor
CPW	coplanar waveguide
CVD	chemical vapor deposition
DFT	density functional theory
DUT	device under test
EBSD	electron backscatter diffraction
EM	electromagnetic
FDSOI	fully depleted silicon-on-insulator
FE	ferroelectric
FeFET	ferroelectric field effect transistor
FEL	ferroelastic
FEM	finite element modelling
FEoL	front-end-of-line
FET	field effect transistor
FORC	first-order reversal curve
FRAM	ferroelecrtic random access memory
GaAs	gallium arsenide
GIXRD	grazing-incidence X-ray diffraction
GSG	ground-signal-ground
HZO	hafnium zirconium oxide

IC	integrated circuit
ID	interdigitated
IDC	interdigitated capacitor
IMD	inter-metal dielectric
IoT	internet of things
IP	in-plane
IR	infrared
LC	liquid crystal
LNA	linear network analysis
MEMS	microelectromechanical systems
MEoL	middle-end-of-line
MFM	metal-ferroelectric-metal
MIM	metal-isulator-metal
MIMO	multiple input multiple output
mmWave	millimeter-wave
MoM	method-of-moment
MOS	metal-oxide-semiconductor
MOSFET	metal–oxide–semiconductor field effect transistor
MSW	microstrip waveguide
NEMS	nanoelectromechanical systems
NFC	near-field communication
NRD	non-radiative dielectric
OOP	out-of-plane
PCB	printed cicuit board
PDK	product development kit
PG	point group
PP	parallel plate
PS	phase shifter
PUND	positive up negative down
PVD	physical vapor deposition
PZT	lead zirconate titanate
RF	radio frequency
RFIC	radio frequency integrated circuit
RFID	radio frequency identification
RTA	rapid thermal annealing
SE	spectroscopic ellipsometry
SEM	scanning electron microscopy
SiGe	silicon-germanium
SoA	state-of-the-art
SOI	silicon-on-insulator

SPICE	simulation program with integrated circuit
TEM	transmission electron microscopy
TEOS	tetraethyl orthosilicate
TiN	titanium nitride
TKD	transmission kikuchi diffraction
UV	ultraviolet
VCO	voltage-controlled oscillator
VLSI	very large scale integration
VNA	vector network analyzer
XPS	X-ray photoelectronic spectroscopy
XRD	X-ray diffraction

List of Symbols

$\vec{B}$	magnetic field induction
B_p	fractional bandwidth
C	capacitance
C_c	Curie constant
$\vec{D}$	dielectric displacement
d	thickness
$\vec{E}$	electric field strength
E_c	electric coercive field strength
F	Gibbs free energy
f	frequency
f_0	center frequency
Δf	absolute bandwidth
FoM^{BPF}	figure of merit of a bandpass filter
FoM^{BPF}_{norm}	normalized figure of merit of a bandpass filter
FoM^{PS}	figure of merit of a phase shifter
FoM^{PS}_{norm}	normalized figure of merit of a phase shifter
$\vec{H}$	magnetic field strength
H_c	magnetic coercive field strength
I	electric current
IL	insertion loss
$\vec{J}$	current density
L	inductance
$\vec{p_i}$	dipole moment
$\vec{P}$	polarization
P_r	remanent polarization
P_s	saturation polarization
Q	quality factor
Q_{BPF}	bandpass filter quality factor
R	resistance
S	scattering parameter

T	temperature
t	time
$\tan\delta$	loss tangent
T_c	Curie temperature
T_0	critical temperature
V	electric voltage
v	volume
V_c	coercive bias voltage
VPF	voltage performance factor
V_{tun}	tuning voltage
X	reactance
Y	admittance
Z	impedance
η	order parameter
κ	extinction coefficient
ε_r	dielectric permittivity
ε'	real dielectric permittivity
ε''	dielectric loss
ε_∞	high-frequency permittivity
ε_s	low-frequency permittivity
ε_0	vacuum permittivity
ε^*	complex permittivity
ρ_c	charge density
σ	conductivity
τ	relaxation time
τ_c	tunability
τ_f	frequency tunability
χ	dielectric susceptibility
$\Delta\phi$	differential phase shift
ω	angular frequency

Contents

Chapter 1

Introduction

Wireless microwave communication and information systems have become ubiquitous in our daily lives, with devices such as smartphones, tablets with WiFi and GPS, contactless payment systems, radio frequency identification (RFID) and near-field communication (NFC) tags, and wireless chargers. As modern society generates ever-increasing amounts of data, there is a growing need for denser data packing, which in the context of wireless systems means increased bandwidth. As a result, new technologies like microwave millimeter and terahertz waves are being introduced and becoming part of the technology standards such as 5th generation mobile network (5G) and internet of things (IoT).

However, as frequencies increase due to the limitations of transmission range, simple obstacles such as trees or cars can easily block the signal. This makes beam steering and methods such as multiple input multiple output (MIMO) essential. Transmitters and receivers need to be placed in close proximity to each other, requiring constant reorientation of the signal's direction. These systems must also be integrated into portable devices, which impose additional requirements such as small size and low power consumption.

To meet these requirements, new components with enhanced performance and new functionalities are necessary. Additionally, these systems need to be more consumer-friendly, adaptable, reconfigurable, and cost-effective. Therefore, research and development efforts are focused on improving component technologies to meet these challenges. In this sense, components based on ferroelectric materials have great potential in the development of wireless microwave communication and information systems. Their major advantage lies in their low dielectric losses at microwave frequencies, making them competitive with conventional complemetary metal-oxide-semiconductor (CMOS) components at frequencies above 20 GHz.

Ferroelectric materials have a long history since their discovery by Joseph Valasek [1] in 1920. After years of research in materials science, device physics, and the demonstration of a large number of laboratory samples, ferroelectric technology for microwave applications is now paving its way into industry and commercial applications. Most representative examples of ferroelectrics, used in radio frequency (RF) and millimeter-wave (mmWave) circuits, are conventional perovskite ferroelectrics like barium strontium titanate (BST) or lead zirconate titanate (PZT) [2].

Despite their potential advantages, conventional perovskite ferroelectrics have a major drawback in their poor compatibility with CMOS integration standards. In many cases, the ferroelectric is used as a substrate in bulk form, and ferroelectric switching is enabled by fringing electric fields from interdigitated structures deposited on top. Such a structure does not comply with any integrated circuit (IC) manufacturing standards and cannot be integrated into an IC as an individual component.

In addition to architectural concerns, a more significant limitation for conventional ferroelectrics arises from contamination rules and thermal budget restrictions common in IC industry. Modern CMOS processes comprise multiple stages that can be broadly classified into the front-end-of-line (FEoL) and back-end-of-line (BEoL). The FEoL typically consists of active CMOS devices grown directly on Si wafers, such as metal-oxide-semiconductor (MOS) diodes and field effect transistors (FETs). The BEoL, on the other hand, typically comprises passive structures such as resistors, capacitors, inductors, and metallic interconnections such as vias and transmission lines. Because highly conductive metals like Cu or Al are used for interconnections and because these metals have the ability to diffuse into silicon and other metals when in contact, the FEoL and BEoL parts are always manufactured as separate devices with their own contamination specifications and thermal budget. Most perovskite varactors contain heavy elements such as Ba or Sr that are not supported by conventional foundries in the BEoL. From a thermal budget perspective, perovskites are also not compatible with the BEoL because they require high annealing temperatures for proper crystallization, which are far higher than 400° C.

Therefore, conventional ferroelectrics are currently lacking the competitive edge when compared to CMOS analogs. However, the landscape is rapidly evolving with the introduction of ferroelectric hafnium oxide HfO_2. Ferroelectricity of HfO_2 was discovered in 2007 by Böescke and firstly published in 2011 [3]. Since then this material gained a lot of interest as a candidate for non-volatile memory applications [4], neuromorphic computing [5,6], microelectromechanical MEMS and nanoelectromechanical systems (NEMS) [7], and energy harvesting [8]. Due to the effect of spontaneous polarization this material can store information after removal of the external electric field, which resulted in the use of HfO_2 in ferroelectric field effect transistors (FeFETs). The ferroelectric switching also results in varying the material's capacitance upon applied bias electric field, which makes it able to use the material as a varactor, a tunable capacitor, which is a passive, tunable circuit element used widely in RF and mmWave networks.

At the outset of this research, the utilization of ferroelectric HfO_2 as varactors had primarily been explored in the literature by the Dragoman group [9–13] with their investigations concentrated on interdigitated hafnium zirconium oxide (HZO) varactors up to 20 GHz. In this work, the key challenges and advancements in exploring the broadband characteristics, including low-frequency, RF, and mmWave properties, of ferroelectric hafnium zirconium oxide varactors in metal-ferroelectric-metal (MFM) configuration for BEoL applications are addressed. The influence of doping, thickness, temperature and electric field cycling on the varactor's performance are shown. Furthermore, the design, simulation, and measurement of its performance in passive RF devices, such as phase shifters and bandpass filters, are undertaken.

Chapter 2

Scope and Organization of the Thesis

The thesis is organized in the following way: Chapter 3 provides an overview of the basic phenomenological principles of dielectric and ferroelectric materials. It specifically focuses on the material properties at RF and mmWave frequencies. In Chapter 4, an introduction to varactors is made, including their classification and properties. The discussion includes the utilization of the varactors in primitive passive devices such as phase shifters and bandpass filters. Additionally, the layout and simulation of these devices are presented demonstrating their performance. Chapter 5 briefly introduces the basic experimental methods for fabrication and structural and electrical characterization. Chapter 6 then delves into the detailed discussion of all experimental analyses.

The primary objectives of this work can be summarized as follows:

1. Fabrication of MFM varactors based on ferroelectric HfO_2 for RF and mmWave applications.

2. Electrical characterization of the obtained MFMs and optimization of doping parameters and tuning range.

3. Design of special structures for microwave frequency characterization (ranging from 1 GHz to 110 GHz).

4. Design and integration of Back-End-of-Line (BEoL) passive RF devices.

Based on these objectives, the presented results in Chapter 6 can be categorized into three parts:

1. Investigation of the characteristics of hafnium zirconium oxide as a material for tunable capacitance applications. This includes low-frequency electrical measurements conducted on test structures with varying thicknesses and doping. Special attention is given to investigating the influence of antiferroelectric-like behavior on tuning capabilities and quality factor. Additionally, the influence of temperature on these properties is examined.

2. RF and mmWave characterization of specific test structures. These structures comprise single varactors deposited directly on Si substrates, patterned using primitive lift-off lithography, as well as more sophisticated BEoL-integrated devices for accurate extraction of material parameters at high frequencies.

3. Design, simulation, and characterization of potential tunable devices based on HfO_2. The main objective is to demonstrate the integration capability of varactors into the BEoL of CMOS technology nodes.

Chapter 3

Fundamentals

In this chapter, the phenomenological and fundamental introduction into the ferroelectric materials and their applications for tunable RF devices is be provided. First, the basic information about tunable ferroelectrics in RF applications is presented, which later will be measured and simulated. Then, the fundamental properties of ferroelectric thin films and their influence on varactor operation are going to be discussed.

3.1 Basics

The behavior of electromagnetic fields and its interaction with the matter is described bt Maxwell's equations [14]:

$$\mathrm{rot}\,\vec{E} = -\frac{\partial}{\partial t}\vec{B}, \tag{3.1}$$

$$\mathrm{rot}\,\vec{H} = \vec{J} + \frac{\partial}{\partial t}\vec{D}, \tag{3.2}$$

$$\mathrm{div}\,\vec{D} = \rho_c, \tag{3.3}$$

$$\mathrm{div}\,\vec{B} = 0, \tag{3.4}$$

where E and $\vec{H}$ describe the electric and magnetic field strength, $\vec{D}$ the dielectric displacement, $\vec{B}$ the magnetic induction, $\vec{J}$ the current density and ρ_c the density of charges. The dielectric displacement describes the state of the free and bound electric charges inside the material. For small electric field strengths $\vec{D}$ can be expressed by

$$\vec{D} = \varepsilon^* \varepsilon_0 \vec{E} = \varepsilon_0 \vec{E} + \vec{P}, \tag{3.5}$$

where ε_0 is the dielectric permittivity of vacuum ($\varepsilon_0 = 8.854 \times 10^{-12}$ V^{-1}m^{-1}), ε^* the complex dielectric permittivity, and $\vec{P}$ the polarization - a macroscopic property, describing the density of the dipole moments $\vec{p_i}$ in the dielectrics:

$$\vec{P} = \frac{1}{v}\sum \vec{p_i}. \tag{3.6}$$

Here, $\vec{p_i}$ is the dipole moment and v the volume. The polarization $\vec{P}$ describes the dielectric displacement which originates from the response of a material to an external field. Hence, it can be defined from Eq. (3.5) as:

$$\vec{P} = \varepsilon_0 \vec{E}(\varepsilon^* - 1) = \varepsilon_0 \vec{E}\chi, \tag{3.7}$$

where $\chi = \varepsilon^* - 1$ is the dielectric susceptibility.

The complex permittivity ε^* is in turn expressed through real and imaginary functions as following:

$$\varepsilon^* = \varepsilon' - \mathrm{i}\varepsilon''. \tag{3.8}$$

ε'' is called dielectric loss and attributes to the dissipation of energy in the material upon its polarization. This imaginary part reflects the delayed response under corresponding external effects. More often the ratio of ε'' and ε' is used which is called the loss tangent $\tan\delta$:

$$\tan\delta = \frac{\varepsilon''}{\varepsilon'}. \tag{3.9}$$

For anisotropic crystals permittivity and dielectric loss are expressed as a second-rank tensor ε_{ij}. The complex permittivity directly relates to the complex refractive index:

$$n^* = n' - \kappa, \tag{3.10}$$

with [15]:

$$\varepsilon^* = n^{*2}, \tag{3.11}$$
$$\varepsilon' = n'^2 - \kappa^2, \tag{3.12}$$
$$\varepsilon'' = 2n'\kappa, \tag{3.13}$$

where κ is the extinction coefficient.

3.1.1 Dielectric response

At high frequency f dielectric materials are interacting differently with an incident electromagnetic (EM) wave, depending on their structure and composition. Depending on the frequency and hence the energy of the EM wave, different mechanisms of interaction are triggered (Fig. 3.1). Each of those interactions lead to a change of the real and imaginary parts of permittivity.

In the ultra-low frequency range (1 Hz - 10 kHz) the oscillation of the EM wave is slow enough to let the space charges (charged defects or impurities at grain boundaries, or ions) to dissipate through the material and form the depletion layer.

In the radio- and microwave range the EM wave frequency reaches the resonance frequency of the polarization reorientation of the dipoles and a so-called dielectric relaxation takes place, manifested in a reduction of the real permittivity ε' and a peak in the imaginary permittivity ε'' or in the loss tangent. Depending on the type of dielectric, there are different types of relaxation mechanisms. The most fundamental one is called Debye relaxation and has a relation [2, 14, 16]:

$$\varepsilon_r = \varepsilon_\infty + \frac{\varepsilon_s - \varepsilon_\infty}{1 + i\omega\tau}, \tag{3.14}$$

$$\varepsilon'(\omega) = \varepsilon_\infty + \frac{(\varepsilon_s - \varepsilon_\infty)}{1 + \omega^2\tau^2}, \tag{3.15}$$

$$\varepsilon''(\omega) = \frac{(\varepsilon_s - \varepsilon_\infty)\,\omega\tau}{1 + \omega^2\tau^2}, \tag{3.16}$$

where ε_s and ε_∞ are the low-frequency and high-frequency permittivities, respectively, τ is the relaxation time and ω is the angular frequency.

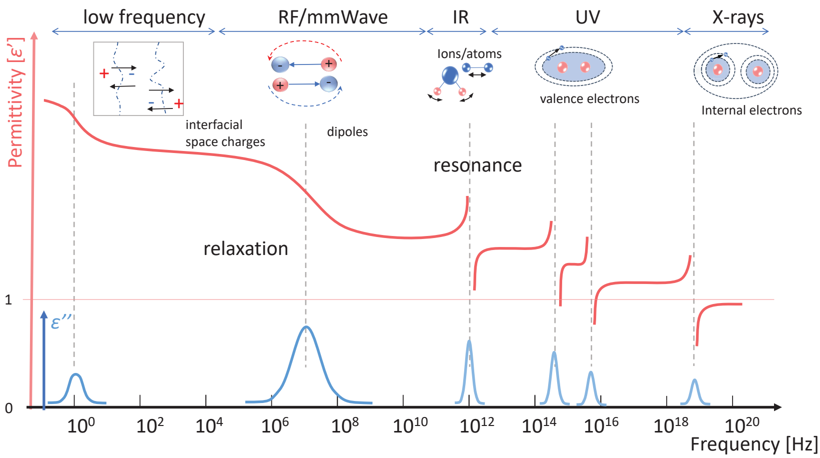

Figure 3.1: Different interaction mechanisms of EM waves with solids in broad frequency spectrum [16, 17].

After the relaxation, going further in the EM spectrum and approaching THz and infrared (IR) frequencies, the dielectrics start to show resonances manifested in a discontinuity in ε' values (Fig. 3.1). This is caused by material's absorption of EM waves due to oscillations of the molecules or atoms in the crystal lattice. Here, the optical properties come into play. The resonances also occur further in the EM spectrum at ultraviolet (UV) frequencies, triggered by the oscillation of valence electrons, which contribute to the polarization. Further in the EM spectrum, approaching extremely high frequencies ($f > 10^{19}$ Hz), the polarizable components of the material, more specifically the electrons on the deep internal level, cannot follow the rapid oscillation of the EM field. At such high frequencies the dielectric permittivity approaches unity (Fig. 3.1) and the absolute permittivity approaches ε_0. Therefore, the material behaves as a vacuum [16].

In this work the emphasis is made on the dielectric response of ferroelectric materials in the RF and mmWave spectrum. In this frequency range, in addition to the relaxation behavior, ferroelectric materials may also show resonance behavior [2, 18]. However, it is necessary to pay attention if the resonance is definitely caused by intrinsic crystalline effects and not by extrinsic effects, like an LCR resonance. The latter is usually caused by electrode or cable inductance. To avoid that, it is necessary to filter out all the parasitic contributions of aforementioned elements. This requires an additional calibration of the setup (see Section 5.4.3) Also, it should be kept in mind that different frequency ranges require specific techniques to measure them.

3.1.2 Loss tangent

The dielectric losses are happening in all dielectric and paraelectric materials. They can be classified with respect to their mechanism into intrinsic and extrinsic losses (Fig. 3.2) [2, 19–24]. The $\tan\delta$ is an additive property [2], i.e the total loss tangent can be described